

---

Erik Jonsson School of Engineering and Computer Science

---

2012-12-10

*A Stacked Polymer Film for Robust Superhydrophobic Fabrics*

UTD AUTHOR(S): Wonjae Choi

©2013 The Royal Society of Chemistry. This article may not be further made available or distributed.

## A stacked polymer film for robust superhydrophobic fabric<sup>†</sup>

Cite this: *Polym. Chem.*, 2013, **4**, 1664

Youngmin Yoo,<sup>a</sup> Jae Bem You,<sup>a</sup> Wonjae Choi<sup>b</sup> and Sung Gap Im<sup>\*a</sup>

A robust superhydrophobic fabric was achieved by depositing a stacked polymer film composed of a poly(1,3,5,7-tetravinyl-1,3,5,7-tetramethylcyclotetrasiloxane) (p(V4D4)) layer and a poly(1*H*,1*H*,2*H*,2*H*-perfluorodecylacrylate) (p(PFDA)) layer. The polymer film was deposited by initiated chemical vapor deposition (iCVD), a solventless process that allows conformal coating of the stacked polymer film on various micro-structured substrates. The two polymeric layers most likely formed a covalent bonding at their interface, and thus the stacked polymer film was characterized by both strong hydrophobicity and enhanced mechanical robustness originated from highly cross-linked p(V4D4) and p(PFDA). The surface topography of superhydrophobic coating was systematically tunable by controlling the operating parameters of iCVD process and a hierarchical structure was obtained by a simple one-step iCVD process. The film was also highly transparent in the wavelength range from 380 nm to 780 nm. Fabrics coated with this stacked polymer film displayed chemical robustness even after exposure to different chemicals including acetone, toluene, H<sub>2</sub>SO<sub>4</sub>, and KOH. The fabric also maintained its water repellency even after 20 000 cycles of the abrasion test and after 75 cycles of the laundry test.

Received 14th November 2012  
Accepted 9th December 2012

DOI: 10.1039/c2py20963b

[www.rsc.org/polymers](http://www.rsc.org/polymers)

### Introduction

The superhydrophobic surface is defined as a surface with a water contact angle higher than 150°. Superhydrophobic surfaces have drawn a great deal of research interest and led to various industrial applications, including water-repellent, self-cleaning, and antifouling surfaces.<sup>1–4</sup> A superhydrophobic surface<sup>5</sup> can be obtained by the combination of the chemical property of low surface energy and the topographical property of the textured surface.<sup>6–14</sup> Both measures of superhydrophobicity – contact angle and hysteresis – are improved as the fraction of the contact area between water and the solid surface decreases. Therefore, a hierarchical structure is highly desirable for a superhydrophobic surface because such a structure can further reduce the contact area between water and solid.<sup>15,16</sup>

Among various industrial applications, superhydrophobic fabrics are of particular interest. Indeed the seminal research by Cassie and Baxter was on waterproof textiles, and since then numerous research groups have reported superhydrophobic textiles.<sup>17–22</sup> While waterproof textiles are commonly used for umbrella or raincoat, commercially available superhydrophobic fabrics are still rare. Superhydrophobic fabrics allow the possibility of ‘breathable’ non-wetting outdoor apparel, which

is a fast growing billion-dollar market. Thus textile industries are still urgently searching for a simple and reliable methodology to produce water-repellent fabrics.

One of the greatest challenges to the commercialization of superhydrophobic fabrics is to secure the long-term stability of the superhydrophobic fabrics under the conditions of our daily use.<sup>23</sup> Porous and hierarchical structures are critically important to imbue the fabric with superhydrophobicity. Unfortunately, such porous, hierarchical structures are vulnerable to various kinds of mechanical stresses, such as scratching, abrasion, and tensile stresses, which are common in our daily life. In addition, a fabric is often exposed to various organic contaminants like greasy dirt in an ordinary outdoor environment. Organic contaminants, due to their low surface tension, can penetrate relatively easily into the porous superhydrophobic surface, and are extremely difficult to remove. The smear of greasy dirt into the texture alters the surface properties of the texture. Removal of such contaminants is usually accomplished by laundry with a detergent, which is, unfortunately, a highly aggressive procedure for the coating layer, as well. Therefore, the development of a coating layer that is resistant to various chemical and mechanical stresses is the key for the commercialization of a superhydrophobic fabric.

Despite the critical importance of chemical and mechanical durability of a superhydrophobic surface, only few methods have been disclosed to address this issue.<sup>24–30,32,33</sup> However, these studies require complicated fabrication methods and their application to mass production is still illusive. For instance, plasma treatment<sup>24</sup> was used to prepare robust

<sup>a</sup>Department of Chemical and Biomolecular Engineering, Korea Advanced Institute of Science and Technology, Daejeon, 305-701, Korea. E-mail: [sgim@kaist.ac.kr](mailto:sgim@kaist.ac.kr)

<sup>b</sup>Department of Mechanical Engineering, University of Texas at Dallas, Texas, USA

† Electronic supplementary information (ESI) available: The schematic image of an entrapped air pocket, SEM and EDS mapping images, contact angle and SEM images after soaking in acid, base and oxidant. See DOI: 10.1039/c2py20963b

superhydrophobic coating due to its simple method. However, the plasma method needs high energy and tends to damage functional groups by reactive species of plasma.<sup>31</sup> The CVD method was also used to improve the durability of the superhydrophobic fabric, but the process is still highly complex.<sup>32</sup> Zhou *et al.* also fabricated a durable superhydrophobic fabric by coating a fluoroalkyl silane modified silicone rubber-nanoparticle composite. This coating shows durable superhydrophobicity.<sup>33</sup>

A superhydrophobic surface had also been obtained by initiated chemical vapor deposition (iCVD) of a hydrophobic fluoropolymer film.<sup>34</sup> A vaporized monomer and an initiator undergo a radical polymerization in the vapor phase *via* the iCVD process. Once vaporized, the initiator molecules are thermally decomposed upon contact with a hot filament to form radicals. The radicals activate the vaporized monomer to initiate the chain reaction. As a result, the deposition of polymer films occurs on the chamber substrate kept at mild temperature (15–40 °C). This process is a one-step, solvent-free process to deposit polymer films conformally onto various complex surface structures of substrates, regardless of the substrate material.<sup>35</sup> Electrospun fiber mats have been coated with a fluoropolymer by the iCVD process, which showed a water contact angle as high as 175°. However, the mechanical and chemical robustness have not yet been investigated with the iCVD superhydrophobic coating. Here, we introduce a new stacked polymer film as a coating layer on a fabric to produce a robust superhydrophobic surface. The proposed film was synthesized simply by a one-step iCVD process, with a mechanically robust organosilicone polymer layer and a hydrophobic fluoropolymer layer. The two layers were adhered to form a stacked polymer structure. The mechanical and chemical robustness of the organosilicone layer reinforced the fluoropolymer layer. By coating a fabric with the stacked polymer film, we successfully obtained a superhydrophobic fabric with an exceptional stability under various, harsh environmental stresses. The stacked polymer-coated fabric was exposed to a variety of mechanical and chemical stresses, such as the incubation in acids, bases, and various organic solvents, heating and freezing, UV-irradiation, ultrasonication, and mechanical abrasion. No noticeable change in the water contact angle on the fabric was observed through these experiments. The superhydrophobic fabric also withstood more than 75 washing cycles in a commercial laundry machine, and thus we believe the reported superhydrophobic fabric can be used for practical long-term applications.

## Experimental section

The deposition of poly(1,3,5,7-tetravinyl-1,3,5,7-tetramethylcyclotetrasiloxane) (p(V4D4)) and poly(1*H*,1*H*,2*H*,2*H*-perfluorodecylacrylate) (p(PFDA)) was performed in a custom-built iCVD reactor (Daeki Hi-Tech Co., Ltd). 1,3,5,7-tetravinyl-1,3,5,7-tetramethylcyclotetrasiloxane (V4D4, Aldrich) and 1*H*,1*H*,2*H*,2*H*-perfluorodecylacrylate (PFDA, Aldrich 98%) monomers were heated to 70 °C, and *tert*-butyl peroxide (TBPO, Aldrich, 98%) used as an initiator was kept at room temperature. V4D4 and TBPO were delivered into the reactor at 0.6 sccm. Flow rates

were regulated by needle valves. The reactor condition was maintained at 200 mTorr. The substrate temperature and filament temperature were held at 35 °C and 200 °C, respectively. After the deposition of p(V4D4), PFDA and TBPO were delivered into the reactor at 0.6 sccm. The reactor pressure, substrate temperature, and filament temperature were maintained at 100 mTorr, 30 °C, and 200 °C, respectively. The film thickness was monitored *in situ* by a He–Ne laser (JDS Uniphase) interferometer. All films were deposited on both sides of 8 cm × 8 cm polyester mesh (Puritech, 100%).

The Fourier transform infrared (FT-IR) and X-ray photoelectron spectroscopy (XPS) were performed with an Alpha FT-IR Spectrometer, BRUKER, and Multilab 2000, Thermo, respectively. Atomic percentage of the fabric surface was obtained from XPS analysis. The structure of the coated fabric was verified using scanning electron microscopy (SEM) (Nova230, FEI) and atomic force microscopy (AFM) (PSIA XE-100). Energy dispersive spectrometer (EDS) elemental mapping was also performed in the course of SEM measurement.

Transmittance was measured by UV/VIS spectroscopy (Shimadzu UV-3600). The contact angle was measured with 5 µL of deionized water droplets, by a contact angle meter (DSA, KRÜSS).

The abrasion test was carried out according to the Martindale method (ISO 12947-2: 1998) using a Nu-Martindale 864 abrasion and pilling tester. The test was carried out with 9 ± 0.2 kPa at a temperature of 20 ± 2 °C and humidity of 45 ± 15%. The thermal test was performed in an oven at 120 °C and a refrigerator at –16 °C. UV resistance was tested in a Minuta technology fusion cure system (MT-UV-A10). The ultrasonication test was performed in a JAC-2010 ultrasonicator. The laundry test was carried out by a laundry machine (LG, WF-TS107A). Laundry cycles were progressed until 75 cycles, each of which is 20 minutes long, comprising standard washing and rinsing steps. Coated fabric was washed in the laundry machine or with a commercial detergent which is a mixture of surfactants, bleaching agents, and other additives (LG healthcare, laundry detergent tech. 1 sheet per cycle).

Acid and base tests were performed by soaking the coated fabric in diluted aqueous solution of sulfuric acid (H<sub>2</sub>SO<sub>4</sub>) (Daejung, >95%) (pH 2) and diluted aqueous solution of potassium hydroxide (KOH) (Aldrich, 90%) (pH 12). The pH of each solution was maintained at 2 for acid and 12 for base, respectively. A strong oxidizing agent, hydrogen peroxide (H<sub>2</sub>O<sub>2</sub>) (Daejung, >30%) was also used to test the stability of superhydrophobic fabrics. Various organic solvents such as acetone, ethanol, tetrahydrofuran (THF), toluene, and isopropyl alcohol (IPA) were also used to test the durability of the superhydrophobic fabric. The coated fabric was soaked in the selected organic solvents for a designated time and dried with N<sub>2</sub> purge. The contact angle was measured with the dried fabric.

## Results and discussion

### Film deposition and robustness

A stacked polymer film was obtained simply by a successive deposition of an organosilicone polymer, p(V4D4) and a

fluoropolymer, p(PFDA) using the iCVD process. To obtain a superhydrophobic surface, p(PFDA) was chosen, since p(PFDA) is a fluorocarbon polymer material with an exceptionally low surface energy ( $9.3 \text{ mN m}^{-1}$ ).<sup>36</sup> It is reported that environmental issues have been raised against perfluorocarbon materials, such as perfluorooctanoic acid, perfluorononanoate, and perfluorodecanoic acid.<sup>37</sup> However, p(PFDA) used in this work is a polymeric material and is strongly bound on the p(V4D4) layer to minimize these environmental issues. The chemical formulae of p(V4D4) and p(PFDA), and a schematic structure of the stacked polymer, p(V4D4-L-PFDA), coated fabric are shown in Fig. 1.

To obtain a stacked polymer film, firstly a homopolymer of p(V4D4) was deposited to form a bottom layer. Once a desired thickness of p(V4D4) was achieved, the next vaporized monomer, PFDA was introduced into the iCVD chamber with V4D4 for 1 minute and the flow of V4D4 monomer was stopped, and the deposition of p(PFDA) was continued to achieve the top layer. During the change of monomer from V4D4 and PFDA, a short period exists when both V4D4 and PFDA were mixed in the iCVD chamber. This short period ensures the strong adhesion at the interface between the bottom p(V4D4) layer and the top p(PFDA) layer and hence, the stacked polymer film was obtained (Fig. 2a). The sequential polymerization to form the stacked polymer film was readily achieved through the *in situ* vapor-phase polymerization process.

An ultrasonication in a water bath was applied to the stacked polymer film on Si wafer for 100 h to confirm the strong adhesion between the two layers; no delamination of the layer was observed. The stacked polymer film and a homogeneous p(PFDA) film on Si wafer and slide glass were annealed at  $120^\circ\text{C}$  for 24 h. While a severe morphological change – mostly dewetting – was observed from the p(PFDA) homopolymer film, no noticeable change was detected from the stacked polymer film (Fig. 2b). From these results, we hypothesized that the strong adhesion between p(PFDA) and the substrate was stemmed from the covalent bonding formed by the successive deposition of the p(V4D4) interlayer and p(PFDA). The enhanced interfacial adhesion of two layers allowed an improved stability of the stacked polymer film against the 24 hour annealing at  $120^\circ\text{C}$ .

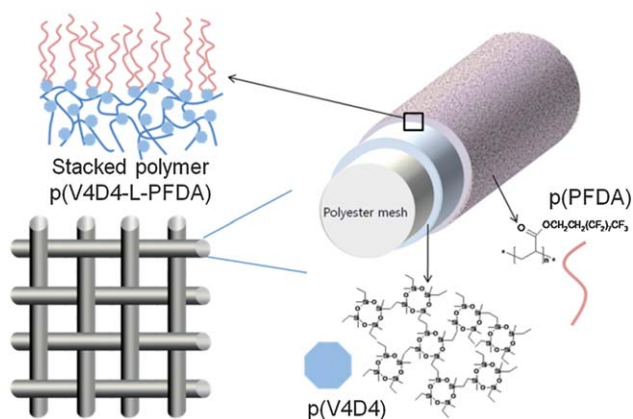


**Fig. 1** A schematic structure of the stacked polymer coated fabric. The stacked polymer is composed of p(V4D4) and p(PFDA).

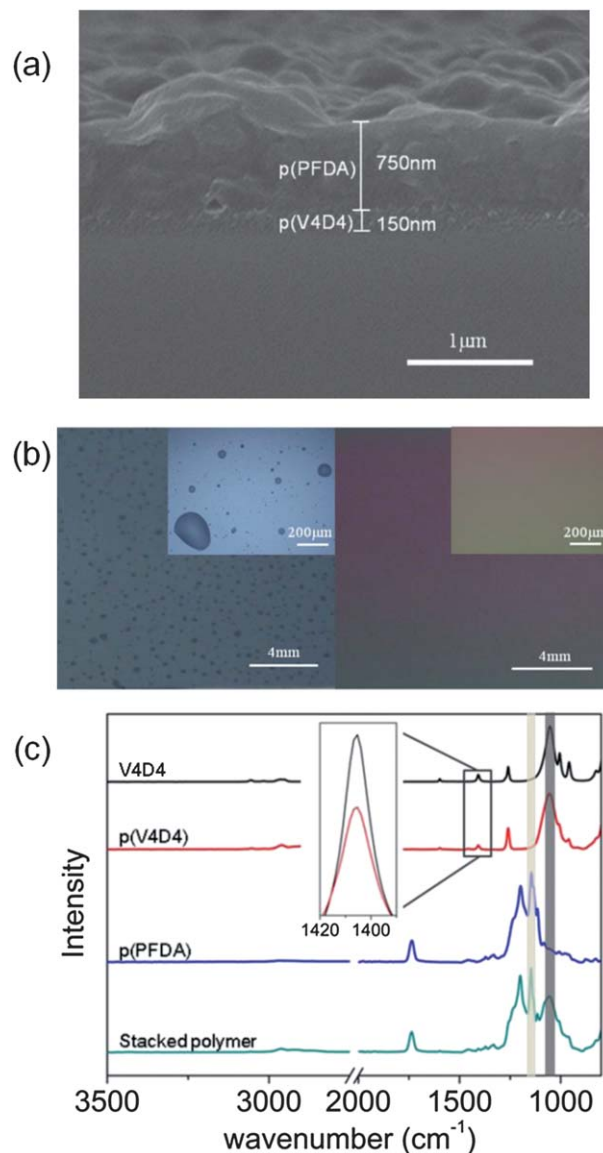


**Fig. 2** (a) The cross-sectional SEM image of p(V4D4-L-PFDA) stacked polymer film on Si wafer. The top layer is p(PFDA), the middle layer is p(V4D4), and the bottom layer is Si wafer. (b) Digital camera images of p(PFDA)-coated Si wafer (left) and p(V4D4-L-PFDA) stacked polymer-coated Si wafer (right) after a thermal treatment at  $120^\circ\text{C}$  for 24 h. Each inset is the enlarged optical microscopy image of each sample. (c) FT-IR spectra for the V4D4 monomer, iCVD p(V4D4) film, iCVD p(PFDA) film, and p(V4D4-L-PFDA) stacked polymer film. Inset shows the magnified image of both V4D4 and p(V4D4) FT-IR spectra at  $1415 \text{ cm}^{-1}$ . The dark gray bar located between  $1065 \text{ cm}^{-1}$  and  $1075 \text{ cm}^{-1}$  represents the asymmetric Si-O-Si stretching peak and the light gray bar located at  $1153 \text{ cm}^{-1}$  represents the  $-\text{CF}_2-\text{CF}_3$  functionality in p(PFDA).

Fig. 2c shows FT-IR spectra of the V4D4 monomer, p(V4D4) deposited iCVD film, p(PFDA) deposited iCVD film, and p(V4D4-L-PFDA) stacked polymer film, respectively. The peak ranging from  $1065 \text{ cm}^{-1}$  to  $1075 \text{ cm}^{-1}$  (Fig. 2c, shaded in dark gray) that corresponds to the asymmetric Si-O-Si stretching peak from the cyclic siloxane ring was detected in both V4D4 monomer and p(V4D4) spectra, which indicates that the iCVD process does not damage the cyclic siloxane ring. The  $1153 \text{ cm}^{-1}$  peak (Fig. 2c, shaded in light gray) represents the  $-\text{CF}_2-\text{CF}_3$

functionality in p(PFDA). The FT-IR spectrum of the stacked polymer contains peaks between  $1065\text{ cm}^{-1}$  and  $1075\text{ cm}^{-1}$ , and at  $1153\text{ cm}^{-1}$ , which confirms both Si–O–Si and  $-\text{CF}_2-\text{CF}_3$  groups were successfully incorporated in the stacked polymer film. The peak intensity at  $1415\text{ cm}^{-1}$  of the V4D4 monomer was decreased to about a half in the spectrum of p(V4D4). This peak represents the vinyl ( $\text{CH}_2=\text{CH}-$ ) group and the decrease of the peak intensity indicates that the V4D4 monomer was polymerized to p(V4D4) by consuming vinyl functionality, but a significant amount of the vinyl group still remained in the polymer. A V4D4 monomer contains 4 vinyl groups and the complete consumption of the vinyl group by free radical polymerization was shown to be impossible due to the steric hindrance.<sup>38</sup> The unreacted vinyl groups in p(V4D4) could also contribute to the formation of the covalent bond with the following PFDA during the deposition of p(PFDA), which also supports the strong adhesion between the p(V4D4) and p(PFDA) layers.

### Superhydrophobicity

The stacked polymer coating converted the hydrophilic fabric to superhydrophobic. The surface of the uncoated fabric was smooth (Fig. 3a). A drop of aqueous blue ink immediately wetted the polyester mat (Fig. 3a inset). The vapor-deposited stacked polymer film conformally covered the hydrophilic fabric by the iCVD process, and the micrometer-scale textured morphology of the fabric was intact. The polyester fabric comprised inter-woven bundles of fibers, and the polymer-coated fabric displayed water-repellency (Fig. 3b inset) with the measured static water contact angle of higher than  $154^\circ$  (Fig. 3b).

High contact angle alone is not a sufficient metric for superhydrophobicity. Surfaces display non-stickiness when the fraction of solid–liquid contact area is small.<sup>39</sup> Fig. 3b shows that the surface of the polyester fiber was roughened slightly by the application of iCVD deposited stacked polymer film. However, this nano-scale texture is not rough enough to entrap additional pockets of air, and water droplets get in contact with a significant fraction of the fabric surface (Fig. S1 in ESI†). At the point of contact between water and the fibers, the water droplet was pinned and consequently, the stickiness of the surface remained significant (see the adhesion between the water droplet and the surface in the inset of Fig. 3b).

The crystallinity of the polymer was reported to increase at lower substrate temperature in the iCVD process.<sup>40</sup> By lowering the substrate temperature from  $40^\circ\text{C}$  to  $30^\circ\text{C}$  during the iCVD process, nanometer-scale crystalline aggregates of p(PFDA) could be formed, which resulted in the roughened surface structure of the stacked polymer film (Fig. 3c). In other words, the iCVD process is capable of tuning the surface roughness of the stacked polymer film by controlling the process parameters of the iCVD process.<sup>41</sup> When this nanometer-scale morphology of the polymer film from the iCVD process was incorporated into the micron-scale textured fabric, a hierarchical structure was easily obtained (Fig. 3c). The digital camera image (Fig. 3c inset) shows a water droplet in the receding phase, confirming that the stickiness of the fabric surface was negligible.

The surface roughness of the superhydrophobic stacked polymer film was monitored by AFM (Fig. 3d–f). The same films used in Fig. 3b and c were deposited on Si wafer at the same batch of the iCVD process, and the AFM images of samples are shown

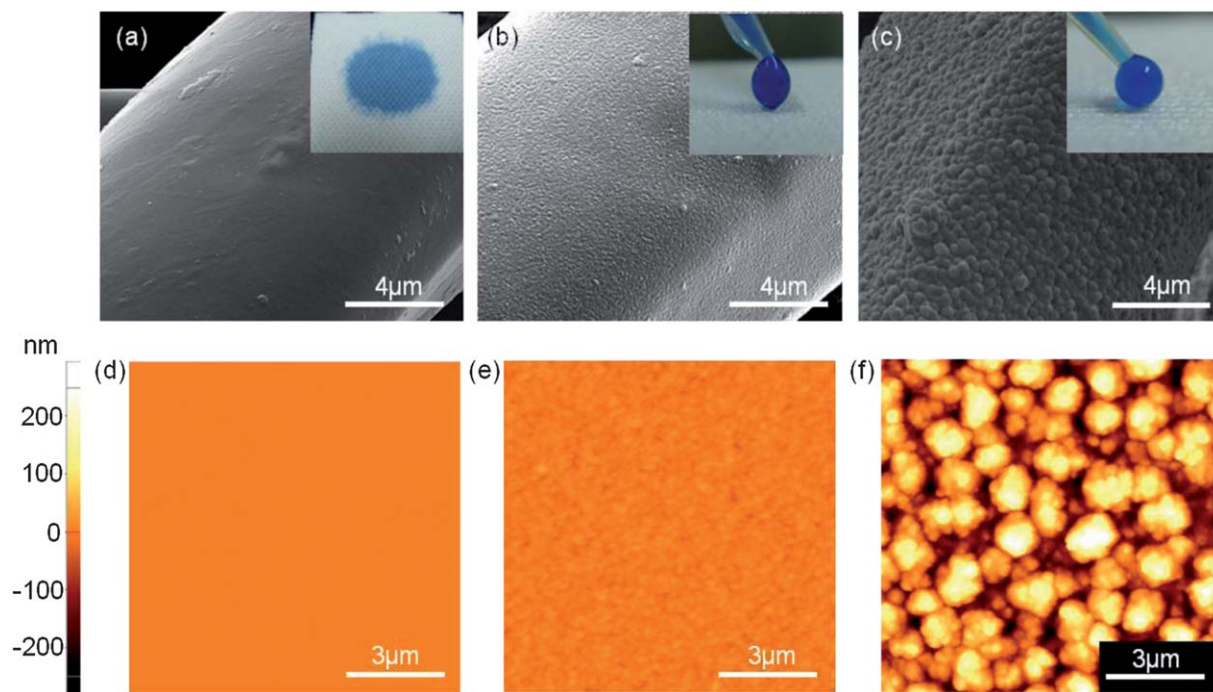


**Fig. 3** (a), (b), and (c) SEM images of the non-coated polyester fabric surface, the slightly rough p(V4D4-L-PFDA) stacked polymer-coated fabric surface, the rougher surface of the p(V4D4-L-PFDA) stacked polymer coated fabric, respectively. Inset images show the hysteresis between a water droplet and a fabric. (d), (e), and (f) represent AFM images of Si wafer obtained from the same experiment batch as the fabrics shown in (a), (b), and (c), respectively.

in Fig. 3e and f. The reference Si wafer surface was extremely smooth and root-mean square (RMS) roughness was 0.14 nm (Fig. 3d). The measured RMS surface roughness of the film significantly increased from 11 nm (Fig. 3b) to 95 nm (Fig. 3c). The additional hierarchical nanostructure on the fabric surface greatly improved the superhydrophobicity of the fabric.

### Optical properties

One of the most desirable properties of the stacked polymer film deposited by the iCVD process is the conformal coverage on various substrates with highly complicated morphologies. Fig. 4a shows the SEM images of the bare polyester fabric (left) and the fabric coated with the stacked polymer film (right). The diameter of each polyester fiber was about 20  $\mu\text{m}$ . No apparent difference was observed and the detailed structure of the texture was clearly maintained after the stacked polymer film was deposited on the fabric. The EDS analysis confirmed that the surface of the fabric was conformally covered with the superhydrophobic stacked polymer film (Fig. S2 in ESI†). The EDS elemental mapping image shows that the fluorine element was conformally deposited on the fabric surface.

The vapor-deposited stacked polymer film showed good optical transparency in the range of visible light. The transmittance of the stacked polymer film was measured at least higher than 98% over the wavelength range of 380–780 nm with the thickness of 700 nm of the stacked polymer film and no

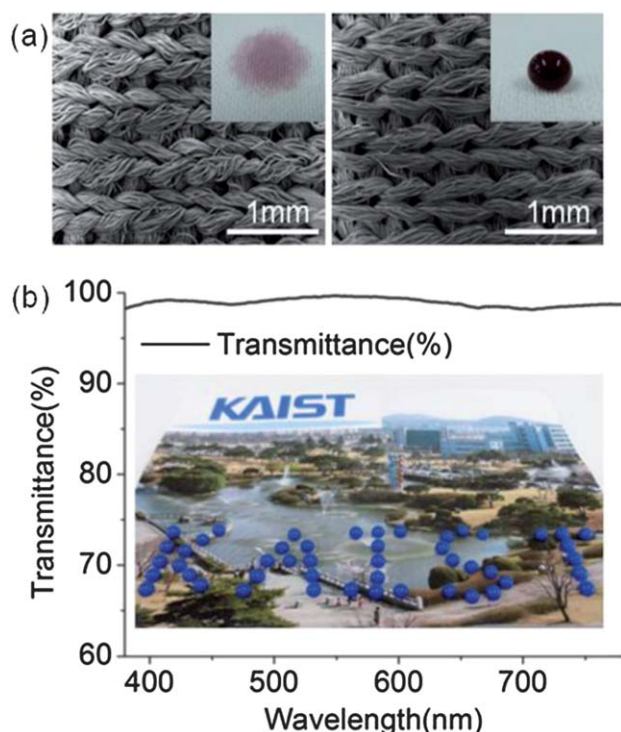


**Fig. 4** (a) SEM images of a pristine (left) and a p(V4D4-L-PFDA) stacked polymer-coated polyester fabric (right). (b) Transmittance of a 700 nm thick p(V4D4-L-PFDA) stacked polymer coated PET film. Both groups of inset images of (a) and (b) are digital camera images which show that the substrate maintains the same feature and color but displays superhydrophobicity after p(V4D4-L-PFDA) stacked polymer coating.

noticeable change of color was observed after the coating process (Fig. 4b). The high transmittance is ascribed to the small difference in the refractive index of p(PFDA) (1.36–1.37)<sup>34</sup> and p(V4D4) (1.47)<sup>38</sup> layers, and the high optical transparency of each polymer layer. The improved transparency of the superhydrophobic surface is of critical importance for the applications such as car window, goggles, and touch screens. Since the coating process is not affected by the chemical nature of the surface of the substrate, and the process does not alter the initially designed color of the substrate, the selection of color for outer apparel will not be restricted by the coating process.

### The durability of superhydrophobicity against chemical and mechanical stresses

The combination of p(V4D4) film and p(PFDA) film by sharing the role of the improved stability and the superhydrophobicity allowed for an extraordinary resistance to various external stresses usually found in our daily life. We evaluated the durability of the superhydrophobic fabrics against annealing, sonication, and incubation in various organic solvents, acids, bases, abrasion, and laundry processes. The stacked polymer-coated fabric was exposed to extremely hot (120 °C) and cold (−16 °C) environments for 40 days and the superhydrophobicity of the fabric remained unchanged (Fig. 5a). The receding contact angles of each fabric exposed to hot and cold environments were  $152.5 \pm 1.7^\circ$  and  $155.5 \pm 2.6^\circ$ , respectively. As is shown in Fig. 2b, p(PFDA) is vulnerable to the thermal stress and the film dewetted during heat treatment. However, the p(PFDA) layer adhered on the surface of p(V4D4) could maintain the morphology due to the restriction of mobility of the p(PFDA) chain in the stacked polymer structure.

Ultrasonication was applied to the superhydrophobic fabric in water for more than 4 days and the superhydrophobic film

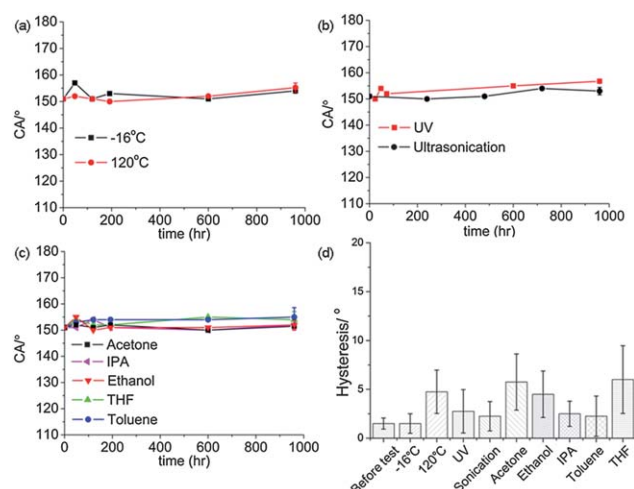


**Fig. 5** Contact angle changes after the chemical and mechanical stresses. (a) Contact angle changes after the thermal test at 120 °C and −16 °C. (b) Contact angle changes with UV irradiation and the ultrasonication test. (c) Contact angle changes with various solvents test (acetone, IPA, ethanol, THF, and toluene). (d) The hysteresis graph of a p(V4D4-L-PFDA)-coated polyester fabric before and after thermal, sonication, UV, and organic solvent tests.

remained intact, which confirms the strong adhesion between the stacked polymer film and the fabric (Fig. 5b). The receding contact angle of the fabric tested with ultrasonication was  $156 \pm 1.6^\circ$ . The same fabric did not lose superhydrophobicity after the irradiation of high intensity ultraviolet (UV) light ( $15 \text{ mW cm}^{-2}$ ) (Fig. 5b). UV irradiation is common in our daily life, mostly when the sample is exposed to outer sunlight. The receding contact angle was  $153.5 \pm 1.3^\circ$ , which supports the robustness of the stacked polymer film against UV exposure. The solar UV irradiation causes degradation of polymer films accompanied by color change. The stacked polymer film showed an exceptional resistance to the UV irradiation possibly due to the highly cross-linked structure of p(V4D4).

The stacked polymer film was highly resistive to the attack of many kinds of organic solvents. Even after 40 days of incubation in toluene, acetone, ethanol, THF, and IPA, the superhydrophobicity of the stacked polymer coated fabric was not degraded (Fig. 5c). The receding contact angles of the samples after incubation in the organic solvents were also higher than  $150^\circ$ . The observation above clearly confirms that the p(V4D4-L-PFDA) coated polyester fabric maintained its superhydrophobicity after the exposure to various harsh environments.

Fabrics coated with the stacked polymer film were also exposed to strong acid ( $\text{H}_2\text{SO}_4$  water solution, pH 2), strong base (KOH water solution, pH 12), and a strong oxidant,  $\text{H}_2\text{O}_2$  for 24 h per test (Fig. S3 in ESI<sup>†</sup>). The superhydrophobicity remained unaffected in all cases. The contact angle was higher than  $150^\circ$  and the contact angle hysteresis was less than  $10^\circ$ .

To check the robustness of the stacked polymer film against laundry processes, the fabric was put into a commercial laundry machine and made to undergo standard washing cycles with the detergent. The laundry machine is specifically designed to induce vigorous, turbulent flows through a combination of intensive rotation and vibration of the wash tray. Such a mechanical agitation, in conjunction with various chemicals in the detergent, offers an extremely harsh environment for superhydrophobic fabrics. Fig. 6a shows the contact angle change, monitored according to the number of laundry cycles. The test was performed for 75 cycles. The water contact angle after 75 laundry cycles was still higher than  $150^\circ$ . XPS (Table 1) analysis indicates that the F element is detected from the fabric after 50 laundry cycles. A quantitative analysis of XPS spectra indicates that atomic percentage of the F element slightly decreased. In addition, the increase of atomic percentage of the Si element was also detected. The observation suggests that the frictional wear of p(PFDA) occurred to expose the surface of p(V4D4). However, the p(PFDA) still remained tethered on the surface of p(V4D4), maintaining the hydrophobicity of the fabric after the laundry test. The SEM image of the fabric surface after the laundry test (Fig. 6c) also shows that hierarchical nanostructure was mostly preserved after the laundry test. The laundry-compatibility of the stacked polymer-coated fabric is of great importance for the fabric to maintain long-term superhydrophobicity. One of the greatest sources of the degradation of superhydrophobicity is the fouling of the surface by organic contamination. In general, the organic contamination is hardly washable by water, and a laundry cycle with a detergent is

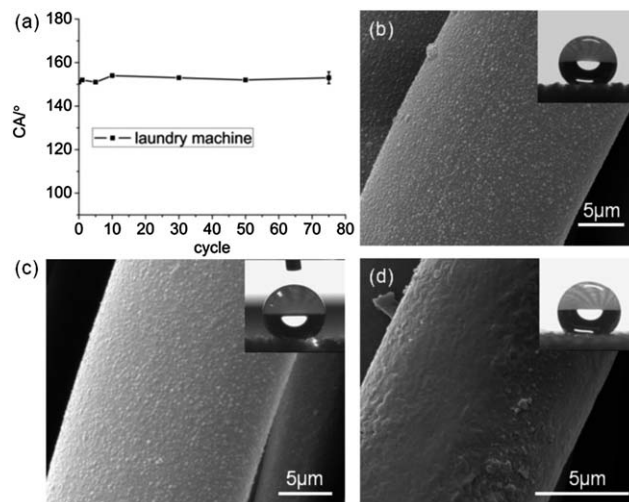


**Fig. 6** (a) Water contact angles plotted with respect to the number of laundry cycles. (b) SEM image of the stacked polymer film coated polyester fabric surface. (c) SEM image of the fabric surface after the laundry test. (d) SEM image of the fabric surface after the abrasion test. Inset images show the shapes of water droplets on each fabric surface.

**Table 1** Atomic percentage of the p(V4D4-L-PFDA) coated fabric surface before and after the laundry cycle (atomic%)

Element	Carbon	Oxygen	Silicon	Fluorine
Before laundry	40.46	6.31	0.84	52.39
After laundry	45.87	8.07	1.08	44.08

necessary to remove the greasy oil contaminants from the surface of the fabric. As discussed above, a laundry cycle itself is a highly aggressive process that applies heavy stress on the fabric, typically leading to the compromise of superhydrophobicity. Since the stacked polymer film is compatible with repetitive laundry cycles, the fouled surface with oil contaminants can be regenerated by 'washing out' oily contaminants out of the fabric.

In order to measure the durability against the mechanical stress, a standard procedure of the abrasion test was performed to a stacked polymer-coated fabric, according to the method of ISO 12947-2:1998 using a Martindale tester. The applied pressure was  $9 \pm 0.2 \text{ kPa}$  and the number of test cycles was 20 000. Fig. 6d shows SEM image after the abrasion test. Although the nanoscale surface protrusions were partially damaged after the 20 000 cycles of the abrasion test, the static water contact angle was  $153 \pm 1.7^\circ$  and the hysteresis was  $18 \pm 3.9^\circ$  even after the abrasion test (Fig. 6d, inset). The observation is ascribed to the p(PFDA) layer that remained adhered on the p(V4D4) layer even after 20 000 cycles of the abrasion test.

The superhydrophobic property of the stacked polymer film mostly stems from the top p(PFDA) layer of the stacked polymer film. The bottom layer of p(V4D4) is to improve the mechanical and chemical stability of the superhydrophobic surface. In general, to improve the mechanical stability of the film, the film must be strongly adhered to the surface of the fabric. The

conventional method to increase the adhesion is to form a chemical bonding between the coating layer and the substrate, but the drawback is the fact that the bonding strength changes depending on the chemistry of the substrate. The p(V4D4) layer deposited through the iCVD process does not form a chemical bonding with the surface of the fabric. Instead, the iCVD process allows the layer to form a conformal contact over the entire perimeter of each interwoven polyester fiber bundle.<sup>42</sup> It is well-known that the adhesive energy increases with the interfacial area of two surfaces.<sup>43</sup> In the case of the stacked film on the fiber bundle, the real surface area of the fabric is much larger than the apparent surface area. The contact area between the iCVD coating and the fiber bundle is enormously large, compared to the apparent surface area of the fabric, and hence the adhesion strength of the iCVD coating on the substrate can be greatly increased. Moreover, the iCVD process is applicable to various kinds of the substrate materials without any surface treatment,<sup>44</sup> which is greatly advantageous over the conventional methods of surface treatment with fluorosilane reagents.<sup>45</sup> The highly cross-linked p(V4D4) film showed extraordinary mechanical robustness and superior thermal stability to the p(PFDA) film, and the stability of the p(PFDA) film is reinforced by p(V4D4) through the adhesion between the two layers.

## Conclusions

In summary, a dramatic increase in the durability against mechanical and chemical stresses of superhydrophobic fabric was achieved by adding the p(V4D4) layer that strongly binds superhydrophobic p(PFDA) to the textured fabrics *via* a one-step, solventless iCVD process. The chemical composition of the stacked polymer p(V4D4-L-PFDA) was confirmed by FT-IR spectra. The p(V4D4) layer significantly enhanced the mechanical stability of p(PFDA) as its remaining vinyl groups were able to bind covalently with p(PFDA). By tuning the parameters of the iCVD process, one could easily confer the secondary nanostructure onto the stacked polymer, and such a structure significantly enhanced water repellency of the fabric. The SEM and AFM images support the presence of the hierarchical structure. The robust superhydrophobic fabric showed improved stability to various types of environmental stresses including UV, thermal stress, ultrasonication, and various organic solvents. Abrasion and laundry tests confirmed the robustness of the superhydrophobic coating. The coating process is applicable to various types of substrates without any surface treatment while allowing enhanced adhesion between the coated film and the substrate. We believe that the robust superhydrophobic coating *via* an iCVD stacked polymer film provides a breakthrough for the commercialization of self-cleaning and anti-contamination fabrics with sufficient durability against various common environmental stresses.

## Acknowledgements

This work was supported by part by the IT R&D program of MKE/KEIT (Grant no. 10041416, The core technology

development of light and space adaptable new mode display for energy saving on 7 inch and 2 W) by KAIST Institute for the NanoCentury, and by a grant from the Fundamental R&D Program for Technology of World Premier Materials funded by the Ministry of Knowledge Economy, Republic of Korea.

## Notes and references

- 1 A. Synytska, R. Khanum, L. Ionov, C. Cherif and C. Bellmann, *ACS Appl. Mater. Interfaces*, 2011, **3**, 1216–1220.
- 2 D. Oner and T. J. McCarthy, *Langmuir*, 2000, **16**, 7777–7782.
- 3 L. Jiang, Y. Zhao and J. Zhai, *Angew. Chem., Int. Ed.*, 2004, **43**, 4338–4341.
- 4 K. Tsujii, T. Yamamoto, T. Onda and S. Shibuichi, *Angew. Chem., Int. Ed.*, 1997, **36**, 1011–1012.
- 5 A. Lafuma and D. Quere, *Nat. Mater.*, 2003, **2**, 457–460.
- 6 H. Gau, S. Herminghaus, P. Lenz and R. Lipowsky, *Science*, 1999, **283**, 46–49.
- 7 N. L. Abbott, J. P. Folkers and G. M. Whitesides, *Science*, 1992, **257**, 1380–1382.
- 8 P. Lenz, *Adv. Mater.*, 1999, **11**, 1531–1534.
- 9 P. Aussillous and D. Quere, *Nature*, 2001, **411**, 924–927.
- 10 K. R. Shull and T. E. Karis, *Langmuir*, 1994, **10**, 334–339.
- 11 M. H. Hui and M. J. Blunt, *J. Phys. Chem. B*, 2000, **104**, 3833–3845.
- 12 S. Abbott, J. Ralston, G. Reynolds and R. Hayes, *Langmuir*, 1999, **15**, 8923–8928.
- 13 D. Yoo, S. S. Shiratori and M. F. Rubner, *Macromolecules*, 1998, **31**, 4309–4318.
- 14 S. G. Im, D. Kusters, W. Choi, S. H. Baxamusa, M. C. M. V. de Sanden and K. K. Gleason, *ACS Nano*, 2008, **2**, 1959–1967.
- 15 L. C. Gao and T. J. McCarthy, *Langmuir*, 2006, **22**, 2966–2967.
- 16 K. Koch, B. Bhushan, Y. C. Jung and W. Barthlott, *Soft Matter*, 2009, **5**, 1386–1393.
- 17 H. X. Wang, J. Fang, T. Cheng, J. Ding, L. T. Qu, L. M. Dai, X. G. Wang and T. Lin, *Chem. Commun.*, 2008, 877–879.
- 18 L. L. Wang, X. T. Zhang, B. Li, P. P. Sun, J. K. Yang, H. Y. Xu and Y. C. Liu, *ACS Appl. Mater. Interfaces*, 2011, **3**, 1277–1281.
- 19 C. Pereira, C. Alves, A. Monteiro, C. Magen, A. M. Pereira, A. Ibarra, M. R. Ibarra, P. B. Tavares, J. P. Araujo, G. Blanco, J. M. Pintado, A. P. Carvalho, J. Pires, M. F. R. Pereira and C. Freire, *ACS Appl. Mater. Interfaces*, 2011, **3**, 2289–2299.
- 20 H. F. Hoefnagels, D. Wu, G. de With and W. Ming, *Langmuir*, 2007, **23**, 13158–13163.
- 21 Y. Y. Liu, R. H. Wang, H. F. Lu, L. Li, Y. Y. Kong, K. H. Qi and J. H. Xin, *J. Mater. Chem.*, 2007, **17**, 1071–1078.
- 22 K. Ramaratnam, V. Tsyalkovsky, V. Klep and I. Luzinov, *Chem. Commun.*, 2007, 4510–4512.
- 23 J. P. Youngblood and N. R. Sottos, *MRS Bull.*, 2008, **33**, 732–741.
- 24 B. Balu, V. Breedveld and D. W. Hess, *Langmuir*, 2008, **24**, 4785–4790.
- 25 J. Zimmermann, F. A. Reifler, G. Fortunato, L. C. Gerhardt and S. Seeger, *Adv. Funct. Mater.*, 2008, **18**, 3662–3669.
- 26 B. Deng, R. Cai, Y. Yu, H. Q. Jiang, C. L. Wang, J. A. Li, L. F. Li, M. Yu, J. Y. Li, L. D. Xie, Q. Huang and C. H. Fan, *Adv. Mater.*, 2010, **22**, 5473–5477.



- 27 H. X. Wang, Y. H. Xue, J. Ding, L. F. Feng, X. G. Wang and T. Lin, *Angew. Chem., Int. Ed.*, 2011, **50**, 11433–11436.
- 28 X. Deng, L. Mammen, Y. F. Zhao, P. Lellig, K. Mullen, C. Li, H. J. Butt and D. Vollmer, *Adv. Mater.*, 2011, **23**, 2962–2965.
- 29 Y. Zhao, Z. G. Xu, X. G. Wang and T. Lin, *Langmuir*, 2012, **28**, 6328–6335.
- 30 T. Verho, C. Bower, P. Andrew, S. Franssila, O. Ikkala and R. H. A. Ras, *Adv. Mater.*, 2011, **23**, 673–678.
- 31 W. E. Tenhaeff and K. K. Gleason, *Adv. Funct. Mater.*, 2008, **18**, 979–992.
- 32 H. Wang, H. Zhou, A. Gestos, J. Fang, H. Niu, J. Ding and T. Lin, *Soft Matter*, 2013, **9**, 277–282.
- 33 H. Zhou, H. Wang, H. Niu, A. Gestos, X. Wang and T. Lin, *Adv. Mater.*, 2012, **24**, 2409–2412.
- 34 M. Gupta and K. K. Gleason, *Langmuir*, 2006, **22**, 10047–10052.
- 35 S. G. Im and K. K. Gleason, *AIChE J.*, 2011, **57**, 276–285.
- 36 M. Ma, Y. Mao, M. Gupta, K. K. Gleason and G. C. Rutledge, *Macromolecules*, 2005, **38**, 9742–9748.
- 37 *Long-Chain Perfluorinated Chemicals (PFCs) Action Plan*, US Environmental Protection Agency, 12/30/2009.
- 38 N. J. Trujillo, Q. G. Wu and K. K. Gleason, *Adv. Funct. Mater.*, 2010, **20**, 607–616.
- 39 D. Quere, *Phys. Stat. Mech. Appl.*, 2002, **313**, 32–46.
- 40 J. Poly, E. Ibarboure, J. Rodriguez-Hernandez, D. Taton and E. Papon, *Macromolecules*, 2010, **43**, 1299–1308.
- 41 A. M. Coclite, Y. J. Shi and K. K. Gleason, *Adv. Funct. Mater.*, 2012, **22**, 2167–2176.
- 42 T. P. Martin, S. E. Kooi, S. H. Chang, K. L. Sedransk and K. K. Gleason, *Biomaterials*, 2007, **28**, 909–915.
- 43 H. Lee, B. P. Lee and P. B. Messersmith, *Nature*, 2007, **448**, 338–341.
- 44 M. E. Alf, A. Asatekin, M. C. Barr, S. H. Baxamusa, H. Chelawat, G. Ozaydin-Ince, C. D. Petruczok, R. Sreenivasan, W. E. Tenhaeff, N. J. Trujillo, S. Vaddiraju, J. J. Xu and K. K. Gleason, *Adv. Mater.*, 2010, **22**, 1993–2027.
- 45 T. Baldacchini, J. E. Carey, M. Zhou and E. Mazur, *Langmuir*, 2006, **22**, 4917–4919.

## Supplementary Information

### A stacked polymer film for robust superhydrophobic fabrics

Youngmin Yoo,<sup>a</sup> Jae Bem You,<sup>a</sup> Wonjae Choi<sup>b</sup> and Sung Gap Im<sup>\*a</sup>

<sup>†a</sup>*Department of Chemical and Biomolecular Engineering, Korea Advanced Institute of Science and Technology, Daejeon, 305-701 Korea. E-mail: sgim@kaist.ac.kr*

<sup>b</sup>*Department of Mechanical Engineering, University of Texas at Dallas, Texas, United States*

1. Schematic image of entrapped air pocket (Fig. S1)
2. SEM and EDS mapping images (Fig. S2)
3. Contact angle and SEM images after soaking in acid, base and oxidant (Fig. S3)

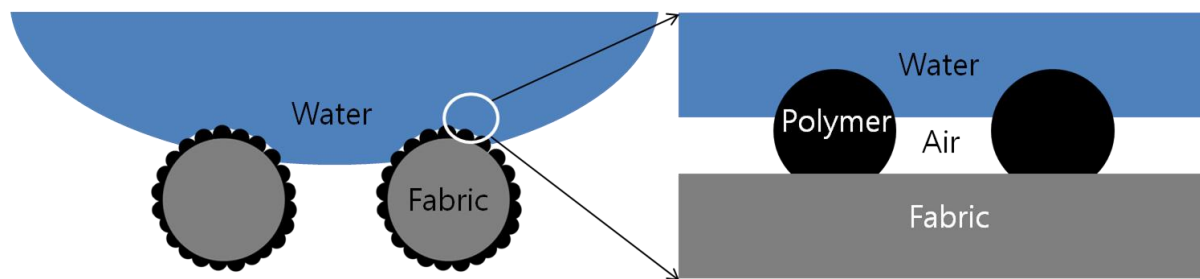


**Fig. S1** A schematic image of entrapped air pocket between the coated fabric and water droplet.

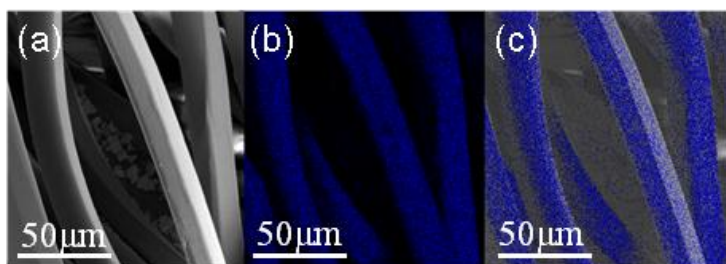


**Fig. S2** (a) SEM image of p(V4D4-L-PFDA) stacked polymer-coated fabric. (b) EDS elemental mapping of fluorine on the same fabric. (c) Merged image of SEM and EDS elemental mapping images.

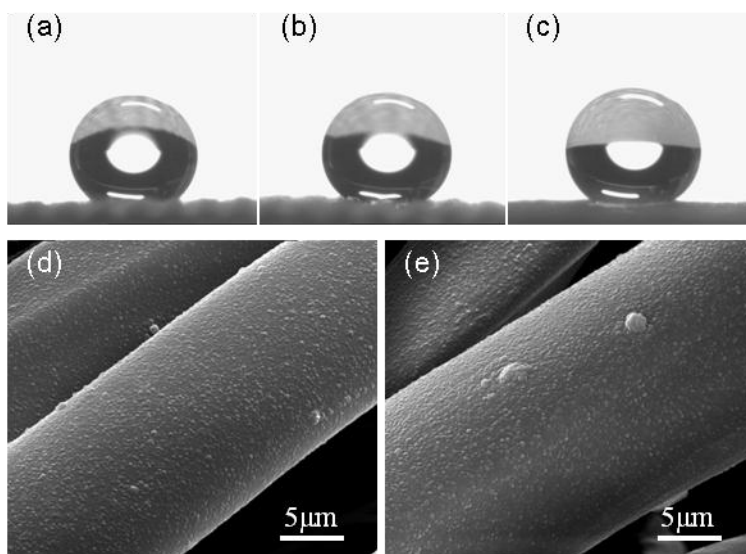


**Fig. S3** (a), (b), (c) Contact angle images of p(V4D4-L-PFDA) coated-polyester fabric after soaking in  $\text{H}_2\text{SO}_4$  (pH 2), KOH (pH 12), and  $\text{H}_2\text{O}_2$  for a period of 24 hrs, respectively. (d), (e) SEM images of p(V4D4-L-PFDA) polyester fabric after soaking in  $\text{H}_2\text{SO}_4$  (pH 2) and KOH (pH 12), respectively.